Molecular structure of an apolipoprotein determined at 2.5-.ANG. resolution

ARTICLE *in* BIOCHEMISTRY · JANUARY 1991

Impact Factor: 3.02 · DOI: 10.1021/bi00217a002

Accelerated Publications

Molecular Structure of an Apolipoprotein Determined at 2.5-Å Resolution[†,‡]

Deborah R. Breiter,[§] Michael R. Kanost,[∥] Matthew M. Benning,[§] Gary Wesenberg,[§] John H. Law,[∥] Michael A. Wells,[∥] Ivan Rayment,[⊥] and Hazel M. Holden*[,§]

Departments of Chemistry and Biochemistry and Institute for Enzyme Research, University of Wisconsin, Madison, Wisconsin 53705, and Department of Biochemistry and Center for Insect Science, University of Arizona, Tucson, Arizona 85721

Received October 29, 1990; Revised Manuscript Received November 26, 1990

ABSTRACT: The three-dimensional structure of an apolipoprotein isolated from the African migratory locust *Locusta migratoria* has been determined by X-ray analysis to a resolution of 2.5 Å. The overall molecular architecture of this protein consists of five long α-helices connected by short loops. As predicted from amino acid sequence analyses, these helices are distinctly amphiphilic with the hydrophobic residues pointing in toward the interior of the protein and the hydrophilic side chains facing outward. The molecule falls into the general category of up-and-down α-helical bundles as previously observed, for example, in cytochrome *c'*. Although the structure shows the presence of five long amphiphilic α-helices, the α-helical moment and hydrophobicity of the entire molecule fall into the range found for normal globular proteins. Thus, in order for the amphiphilic helices to play a role in the binding of the protein to a lipid surface, there must be a structural reorganization of the protein which exposes the hydrophobic interior to the lipid surface. The three-dimensional motif of this apolipoprotein is compatible with a model in which the molecule binds to the lipid surface via a relatively nonpolar end and then spreads on the surface in such a way as to cause the hydrophobic side chains of the helices to come in contact with the lipid surface, the charged and polar residues to remain in contact with water, and the overall helical motif of the protein to be maintained.

Lipids serve important structural and functional roles in all living systems. Consequently, the effective transport of these water-insoluble molecules within the aqueous milieu of the organism is of central biochemical importance. In mammalian systems there exists a diverse array of lipoprotein particles designed for the transport of hydrophobic materials through the blood. These large lipoprotein complexes are believed to be comprised of a nonpolar spherical core of cholesterol esters and triacylglycerols surrounded by a monolayer of phospholipids and cholesterol and a "coat" of apolipoproteins. Within recent years there has been considerable speculation concerning those structural motifs of the apolipoproteins that allow them to interact with both a lipid surface and the lipid-free aqueous environment of the blood. It has been suggested that amphiphilic helices play a key role in such protein–lipid interactions (Segrest, 1974) although until now there has been a lack of high-resolution three-dimensional information concerning apolipoproteins and these putative secondary structural elements.

Like mammals, insects have also solved the problem of lipid transport by the use of lipoproteins. Insects, however, have only one major lipoprotein complex referred to as lipophorin (Shapiro et al., 1988). This particle is typically comprised of 60% protein and 40% lipid (Chino et al., 1981). The two integral protein constituents of lipophorin are apolipophorin I and apolipophorin II with molecular weights of approximately 250 000 and 80 000, respectively (Shapiro et al., 1984; Kanost et al., 1990). In some insects, such as the African locust *Locusta migratoria* and the sphinx moth *Manduca sexta*, there is another small apolipoprotein designated as apolipophorin III (apoLp-III) with a typical molecular weight of 18 000–20 000 (Kawooya et al., 1984; Van der Horst et al., 1984; Chino & Yazawa, 1986). The major function of apoLp-III is to assist in the delivery of lipid from the fat body to flight muscles during prolonged flight. In this process lipid leaves the fat body and associates with lipophorin in the hemolymph. ApoLp-III, which exists as a free monomer in the hemolymph of the resting insect, binds to exposed hydrophobic patches on the surface of the expanding lipoprotein particle and permits the loading of additional lipid (Kawooya et al., 1984, 1986; Wells et al., 1987). On the basis of the observation that apoLp-III bound to a lipid surface occupies an area which is more than twice the area which would be predicted from its molecular dimensions determined from hydrodynamic measurements, it has been suggested that apoLp-III undergoes a large conformational change when binding to lipophorin (Kawooya et al, 1986; Wells et al., 1987).

ApoLp-III isolated from the sphinx moth has been the most extensively studied (Kawooya et al., 1984, 1986; Wells et al., 1987). It is believed to be a prolate ellipsoid with an axial ratio of approximately 3 based on its hydrodynamic properties and its behavior during gel permeation chromatography (Kawooya et al., 1986). The amino acid sequence of the sphinx moth apoLp-III shows similarity to several mammalian apolipoproteins (including apoE, AIV, AI, and CI) and is composed of repeated sequences with amphiphilic helical potential (Cole

[†] This investigation was supported by the following NIH grants: GM29238 to J.H.L., HL39116 to M.A.W., GM41247 to M.R.K., GM351865 to I.R., and HL42322 to H.M.H. D.R.B. was supported by an NIH predoctoral training grant (GM08293). I.R. and H.M.H. are Established Investigators of the American Heart Association.

[‡] Crystallographic coordinates have been submitted to the Brookhaven Protein Data Bank.

* To whom correspondence should be addressed at the Institute for Enzyme Research.

[§] Department of Chemistry and Institute for Enzyme Research, University of Wisconsin.

[∥] Department of Biochemistry and Center for Insect Science, University of Arizona.

[⊥] Department of Biochemistry and Institute for Enzyme Research, University of Wisconsin.

0006-2960/91/0430-603$02.50/0

Table I: Intensity Statistics for Native and Derivative Crystals

	native	potassium tetrabromoaurate(III)	sodium tetrachloro-aurate(III)	trimethyllead acetate	triethyllead acetate	ammonium bromosmate
R_{merge} (%)[a]	4.2	5.3	4.5	6.7	6.7	6.7
total reflections measured	15665	14016	14101	18231	11283	11283
independent reflections	3927	3887	3987	4281	3788	3788
maximum resolution (Å)	3.0	3.0	3.0	3.0	3.0	3.0
average isomorphous differences (%)[b]		28.1	28.2	25.8	39.3	41.7
cell dimensions						
a and *b* (Å)	67.4	67.4	67.2	67.1	67.5	68.2
c (Å)	153.8	153.8	156.9	158.0	154.5	155.3

[a] $R = \sum|I - \bar{I}|/\sum I$. R_{merge} gives the overall agreement between symmetry-related reflections. [b] $R = \sum||F_N| - |F_H||/\sum|F_N|$, where $|F_N|$ is the native structure factor amplitude and $|F_H|$ is the derivative structure factor amplitude.

Table II: Refined Heavy-Atom Parameters[a]

derivative	site no.	relative occupancy	*x*	*y*	*z*	*B*	location
potassium tetrabromoaurate(III)	1	1.9833	0.0919	0.8025	0.0235	52.36	side chain of His 111
	2	2.0853	0.3578	0.8818	0.0640	34.37	between side chains of Gln 13 and Gln 94
	3	3.1052	0.3175	0.8011	0.0758	25.41	side chain of His 24
sodium tetrachloroaurate(III)	1	2.2547	0.1002	0.8022	0.0259	35.64	side chain of His 111
	2	2.3181	0.3619	0.8796	0.0641	40.62	between side chains of Gln 13 and Gln 94
	3	3.2608	0.3212	0.8000	0.0766	33.75	side chain of His 24
trimethyllead acetate	1	2.1000	0.4754	0.9143	0.0676	15.07	side chain of Glu 10
triethyllead acetate	1	1.9452	0.4736	0.9029	0.0595	30.50	side chain of Glu 10
	2	2.0709	0.5933	0.0000	0.0000	30.94	carbonyl oxygen of Leu 30
ammonium bromosmate	1	4.4803	0.4299	0.8433	0.0675	30.66	between side chains of Glu 28 and His 24

[a] *x*, *y*, and *z* are the fractional atomic coordinates; *B* is the thermal factor in Å^2.

et al., 1987). Due to the small size of apoLp-III and the fact that during certain metabolic states it exists as a soluble hemolymph protein, it seemed an ideal apolipoprotein for crystallization trials. Microcrystals of the apoLp-III from the adult sphinx moth were grown, but all attempts to prepare larger crystals for an X-ray analysis were unsuccessful (Holden, unpublished results). However, apoLp-III isolated from *L. migratoria* crystallized readily in a form suitable for a high-resolution structural analysis (Holden et al., 1988), and the cDNA sequence has been determined (Kanost et al., 1988). The molecule contains 161 amino acids with no methionine, tyrosine, or cysteine residues. We describe here the molecular fold of this apolipoprotein as determined by X-ray diffraction analysis. This structure determination is of considerable interest since it represents the first direct visualization of an apolipoprotein.

Experimental Procedures

Crystallization and Preparation of Heavy-Atom Derivatives. Locust apoLp-III was purified according to the method of Kanost et al. (1987). Large single crystals were grown as described (Holden et al., 1988) with 2.8 M ammonium sulfate as the precipitant, buffered with 50 mM potassium/sodium phosphate, pH 7.4. The crystals belong to the space group $P6_522$ with unit-cell dimensions of $a = b = 67.5$ Å, $c = 155.6$ Å, and one molecule in the asymmetric unit.

Isomorphous heavy-atom derivatives were prepared by soaking native crystals for 3–5 days in 3.0 M ammonium sulfate solutions containing either 1 mM potassium tetrabromoaurate (III), 1 mM sodium tetrachloroaurate (III), 20 mM trimethyllead acetate, 2 mM triethyllead acetate, or 5 mM ammonium bromosmate.

X-ray Data Collection and Processing. X-ray data to 3.0-Å resolution were collected from the native crystals and from the heavy-atom derivatives using the Siemens area detector system and the data processing package BUDDHA (Blum et al., 1987). The X-ray source was nickel-filtered copper Kα radiation from a Rigaku RU200 X-ray generator operated at 50 kV and 50 mA. Relevant data collection statistics may be found in Table I. Derivative data sets were scaled to the native data in shells of equal volume in reciprocal space on the basis of resolution.

Higher resolution native X-ray data to 2.4 Å were collected by use of synchrotron radiation and oscillation photography at The National Synchrotron Light Source, Brookhaven National Laboratory. For this X-ray data set an oscillation angle of 1° per film pack was used, and the crystals were rotated about the *c* axis through a net rotation of 60°. The typical exposure time was 2 min per film pack with a crystal-to-film distance of 100 mm. Two crystals were required to collect the X-ray data set which contains 94% of the theoretical number of observations to 2.4-Å resolution. The X-ray films were digitized with an Optronics film scanner and subsequently processed with a set of programs developed by Rossmann (1979) and modified by Schmid et al. (1981). For this native X-ray data set, the average R_{sym} was 3.7%, the average R_{sca} was 3.6%, and R_{merge} was 8.9%, where $R = \sum|I - \bar{I}|/\sum I$, R_{sym} measures the agreement between symmetry-related reflections on the same film, R_{sca} measures the agreement between reflections recorded on successive films in a given film pack, and R_{merge} gives the overall agreement between intensities measured on different films and from different crystals.

Computational Methods. The positions of the heavy-atom binding sites were determined by inspection of the respective difference Patterson maps and placed on a common origin by use of appropriate difference Fourier maps. The origin-removed Patterson function correlation method (Rossmann, 1960; Terwilliger & Eisenberg, 1983) was used to refine the positions, occupancies, and isotropic temperature factors of the heavy-atom sites at 3.0-Å resolution as presented in Table II. Protein phases were calculated by the method of multiple isomorphous replacement. Relevant phase calculation statistics may be found in Table III.

An initial electron density map, using centroid protein phases based on the five heavy-atom derivatives and a structure factor weighting scheme based on the figure of merit, was calculated

Table III: Phase Calculation Statistics[a]

	resolution range							
	∞ to 10.92	6.84	5.34	4.53	3.99	3.61	3.33	3.00
no. of reflections	242	411	495	576	643	702	749	804
figure of merit	0.77	0.70	0.70	0.64	0.58	0.57	0.51	0.47
phasing power [potassium tetrabromoaurate(III)]	2.74	2.83	2.91	2.13	2.23	1.76	1.64	1.45
phasing power [sodium tetrachloroaurate(III)]	2.33	2.71	2.78	2.14	2.32	1.75	1.58	1.50
phasing power (trimethyllead acetate)	0.97	1.22	1.13	0.88	0.91	0.89	0.80	0.79
phasing power (triethyllead acetate)	1.09	1.11	1.06	0.78	0.73	0.88	0.75	0.71
phasing power (ammonium bromosmate)	1.80	1.59	1.46	1.01	0.94	0.97	0.92	1.06

[a] Phasing power is the ratio of the root-mean-square heavy-atom scattering factor amplitude to the root-mean-square lack of closure error (calculated for acentric reflections).

FIGURE 1: Representative portion of the electron density map. The electron density map shown was calculated using X-ray data from 30- to 3.0-Å resolution. Starting from the left, the first amino acid residue shown is Thr 107 followed by Asn, Val, Gly, His, Gln, Trp, Gln Thr, Ser, Gln, and Pro 118. Phe 78 can also be seen in the figure. There are only two tryptophan and two phenylalanine residues in the locust primary sequence, and consequently, these provided ideal "markers" for initiating the fitting of the amino acid sequence into the electron density.

with X-ray data from 30.0 to 3.0 Å. This map was plotted on transparencies and then stacked on thin Plexiglas sheets. The molecular boundaries of the molecule within the crystalline lattice were immediately obvious, and the two tryptophan residues were readily identifiable. Also, the initial map confirmed that the correct space group was indeed $P6_522$ rather than $P6_122$ in that the α-helices were right-handed. With the two tryptophan residues serving as a starting position, a molecular model was fitted to the electron density map by use of an Evans and Sutherland computer graphics system and the molecular modeling program FRODO (Jones, 1985). Several cycles of restrained least-squares refinement of this model first to a nominal resolution of 3.0 Å and then to 2.5 Å have been carried out with the refinement package TNT (Tronrud et al., 1987). The current R factor is 25.0% for all X-ray data between 6.5 and 2.5 Å with root-mean-square deviations from "ideal" geometry of 0.015 Å for bond lengths, 3.1° for bond angles, and 0.007 Å for groups of atoms expected to be coplanar. Details of the refinement will be presented elsewhere upon completion at 2.5-Å resolution.

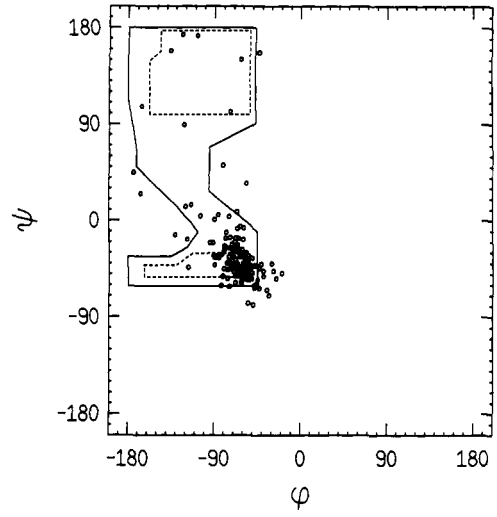

FIGURE 2: Plot of the main-chain dihedral angles. A Ramachandran plot of all non-glycinyl main-chain dihedral angles for the apoLp-III model is shown. Fully allowed ϕ,ψ values are enclosed by dashed lines; those only partially allowed are enclosed by solid lines. As can be seen from consideration of just ϕ,ψ values alone, the apoLp-III structure is almost entirely α-helical.

Results and Discussion

A representative portion of the electron density map calculated to 3.0-Å resolution is shown in Figure 1 and a Ramachandran plot of the main-chain dihedral angles shown in Figure 2. The electron density map was of sufficient quality to allow complete tracing of amino acid residues 7–156. The first six N-terminal and the last five C-terminal amino acid residues appear to be disordered at this stage of the structural analysis. Both Asn 16 and Asn 83, the NH_2-linked glycosylation sites predicted from the cDNA sequence, have rather elongated side-chain densities, making it possible to model into the electron density one N-acetylglucosamine for each residue. The conformation of the five major helices was unambiguous in the original electron density map, but the loops linking these helices were not as well-defined. Consequently, the dihedral angles of the loops will be subject to change as the least-squares refinement of the model is completed to 2.5-Å resolution. However, even at the present stage of model building and refinement, there are many interesting features of the molecule that may be described.

Perhaps one of the most striking aspects of the apoLp-III structure is its elongated appearance, as had been predicted from hydrodynamic studies (Kawooya et al., 1986). The molecule has an overall length of approximately 53 Å and a width of 22 Å. As can be seen from Figure 3, the overall molecular fold of apoLp-III is quite easy to describe. It consists of five long α-helices connected by rather short loops. Those amino acids found in α-helical conformations include residues 7–32 (helix 1), 35–66 (helix 2), 70–86 (helix 3), 95–121 (helix 4), and 129–156 (helix 5). The amino acid sequence determined by Kanost et al. (1988) may be found in Figure 4. This apolipoprotein falls into the category of simple up-and-down helical bundles as described by Richardson (1981). Other members in this category include, for

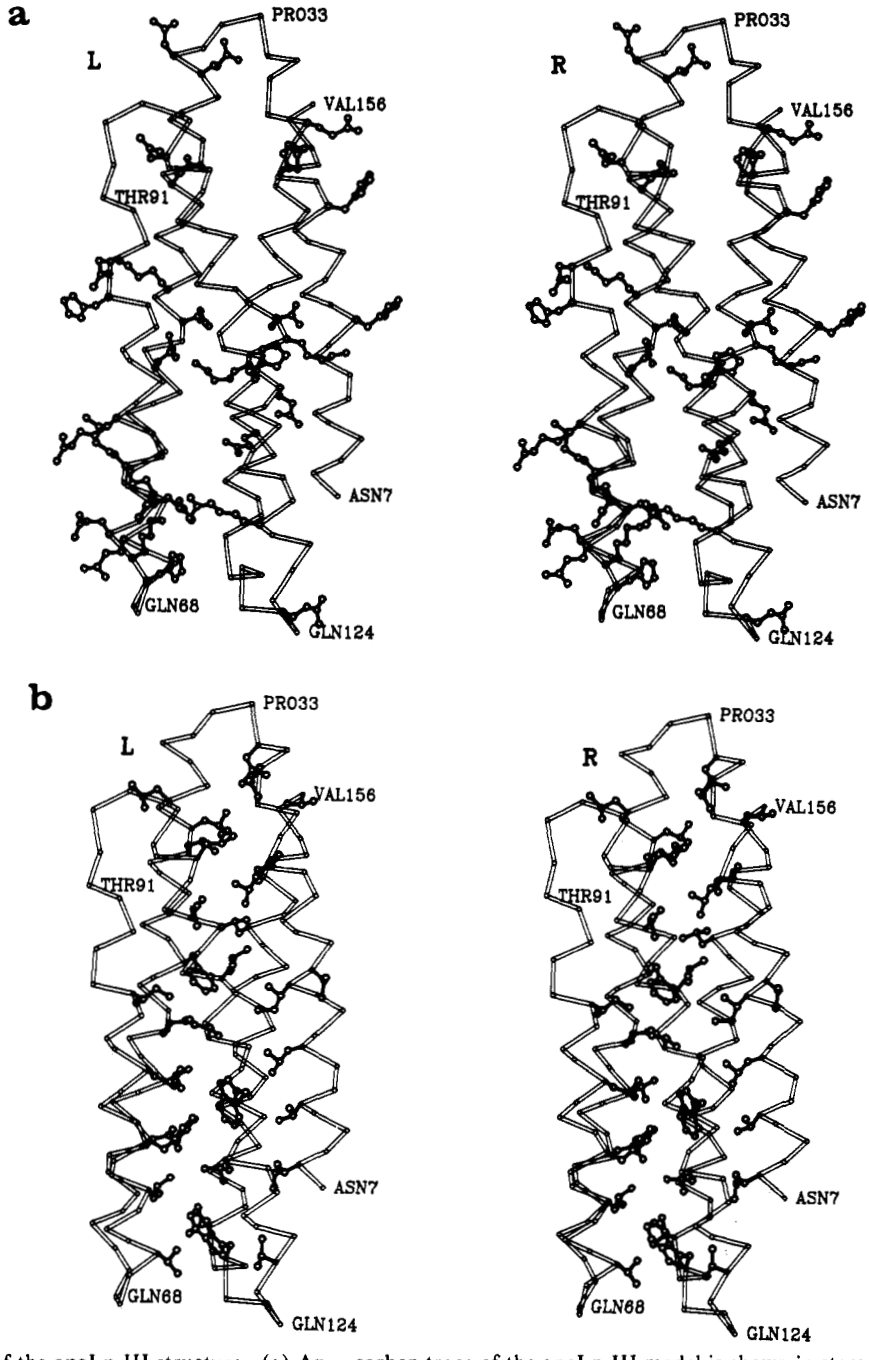

FIGURE 3: Stereoviews of the apoLp-III structure. (a) An α-carbon trace of the apoLp-III model is shown in stereo along with the charged amino acid side chains (His, Glu, Asp, Lys, and Arg). Several of the Cα positions are labeled to aid the reader in following the course of the polypeptide chain. The model begins at Asn 7 and ends at Val 156. The missing residues at the N- and C-termini are not visible at the present stage of the structural analysis. (b) An α-carbon trace of the apoLp-III model is shown in the same orientation as in (a) but with the nonpolar amino acid side chains illustrated (Trp, Phe, Leu, Ile, and Val).

example, myohemerythrin (Hendrickson & Ward, 1977), cytochrome b_{562} (Mathews et al., 1972), and cytochrome c' (Weber et al., 1980).

There are seven proline residues present in the apoLp-III amino acid sequence. Pro 33 is in a loop region, and Pro 159 is not visible in the present electron density map. Three other prolines, namely, residues 35, 95, and 129, serve to delineate the N-termini of helices 2, 4, and 5. Also, in helix 4 there are two prolines residues at positions 118 and 120 with dihedral angles of $\phi = -59°$, $\psi = -51°$ and $\phi = -54°$, $\psi = -37°$, respectively. These ϕ,ψ angles are within the range typical for residues adopting α-helical conformations, and while it is uncommon for prolines to be found in such configurations, it is not without precedence as observed, for example, in lactate dehydrogenase (Abad-Zapatero et al., 1987). The distribution of charged and nonpolar amino acid residues in apoLp-III is shown in Figure 3. Clearly, the helices are amphiphilic with the charged residues facing outward and the hydrophobic residues generally facing toward the interior of the protein. There are several hydrophobic residues, however, pointing toward the solvent (residues 20, 30, and 122). These are located on the same general side of the molecule and may be important for binding to the lipophorin complex.

In the absence of three-dimensional structures for apolipoproteins, several investigators have attempted to use amino acid sequence information to predict how the proteins might bind to a lipid interface (Segrest et al., 1974; Eisenberg et al., 1989). One approach has been to calculate the hydrophobic

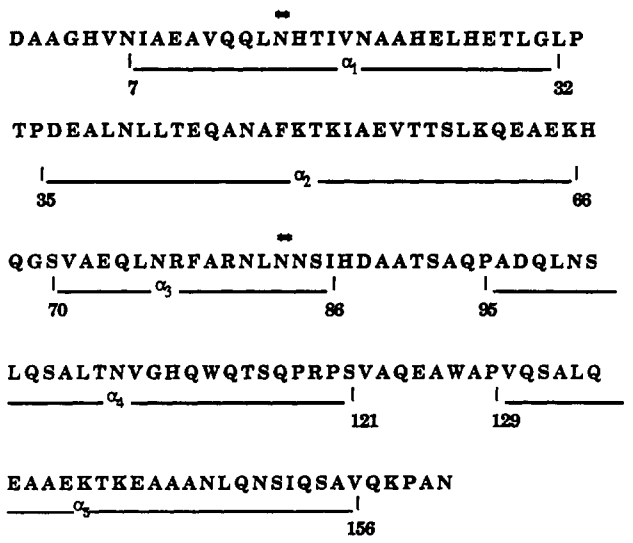

FIGURE 4: Amino acid sequence of apoLp-III from *L. migratoria*. The amino acid sequence shown was taken from Kanost et al. (1988). (**) at Asn 16 and Asn 83 mark the NH_2-linked glycosylation sites. Those residues found in α-helical conformations are indicated below the one-letter code for the amino acids. All other amino acid residues are located in turns.

Table IV: Helical Moments

helix no.	residue no.	average hydrophobicity	hydrophobic moment
1	7–32	0.18	0.40
2	35–66	−0.10	0.36
3	70–86	−0.18	0.71
4	95–121	−0.12	0.30
5	129–156	−0.03	0.40

moment and the hydrophobicity for putative helical segments in apolipoproteins in order to determine whether they might have the potential to bind to a lipid surface. We have calculated the hydrophobic moments and the average hydrophobicity for each of the helices in apoLp-III using the program MOMENT (Eisenberg et al., 1989), and the results are given in Table IV. Helix 3, containing residues 70–86, has the highest helical moment and falls into the category of surface-seeking peptides (Eisenberg et al., 1989). While this helix may have a large hydrophobic moment, it is not a singular entity unto itself but rather associated with four other helices. Consequently, calculation of the individual hydrophobic moments for each helix may not be physically relevant in regard to the biological function of the molecule as a whole. With respect to the entire molecule, however, the α hydrophobic moment is 0.36 with an average hydrophobicity of −0.04, thus placing this protein into the range normally observed for globular proteins.

The molecular fold of apoLp-III described here demonstrates the topological relationship of the α-helical segments and as such provides a structural framework for understanding its biological function as an apolipoprotein. Such information is not available from studies of single synthetic amphiphilic peptides. Given the structure of apoLp-III, it is appropriate to speculate about the mode of interaction of this apolipoprotein with lipophorin. Biophysical studies clearly indicate that apoLp-III unfolds as it forms a monolayer at an air–water interface (Kawooya et al., 1986). Thus, the molecular model described here strengthens the conclusion from previous work (Kawooya et al., 1986; Wells et al., 1987) that apoLp-III must undergo a significant structural change when binding to the lipid surface, since the area occupied by the protein on a lipid surface, estimated to be approximately 3400 Å^2, is considerably greater than the area the molecule would occupy if it was lying on its long axis (approximately 1200 Å^2 based on the crystal structure).

Physiologically, apoLp-III exists in an equilibrium between a soluble monomer and a bound lipoprotein form (Wells et al., 1987). Consequently, it must readily convert from one state to another to carry out its biological function. Thus despite a large change in conformation, the structures of the soluble and bound proteins must be thermodynamically very similar. Therefore any change in the conformation of the protein, such as changes in hydrophobic interactions or hydrogen-bonding patterns, must be accompanied by compensatory effects upon binding to the lipoproteins. The hydrophobic interactions as seen in the interior of the soluble monomer could be compensated for by interactions with lipids. However, any major adjustment to the dihedral angles of the protein backbone would be accompanied by major energetic changes. For this reason it is unlikely that the protein adopts a completely different structure but rather retains most of its secondary structural elements in the same relative orientation with respect to one another.

Previously, we had proposed that the protein initially binds to the lipid surface via one of its ends and then spreads on the surface (Kawooya et al., 1986). The current structure has features which are consistent with this model. As stated above, nearly all the hydrophobic residues are buried between the five helices except for Val 20, Leu 30, and Val 122. In particular, Leu 30 resides in the loop formed between helices 1 and 2. This loop has the sequence TLGLPTP and contains no charged amino acids. It is worth noting that a leucine residue in approximately this position and in the center of a sequence of uncharged amino acids is found in all eight apoLp-III molecules for which complete or partial amino acid sequence data are available (Kanost, unpublished data). In addition, the loop formed between helices 3 and 4 has the sequence AATSAQN and is also uncharged. Thus, this end of the protein is relatively nonpolar and has enough hydrophobic character to be attracted to the lipid surface. As shown schematically in Figure 5, we propose that the protein spreads on the surface by the movement of helices 1, 2, and 5 in one direction and helices 3 and 4 in the other direction around "hinges" located in the loops between helices 2 and 3 (residues 67–69) and between helices 4 and 5 (residues 122–128). This causes the hydrophobic side chains of the helices to come in contact with the lipid surface, the charged and polar residues to remain in contact with water, and the overall helical motif of the protein to be maintained. The surface area for this unfolded form would be at a minimum 2200 Å^2. The role of Val 20, Leu 30, and Val 122 in the binding of apoLp-III to a lipid surface can be tested by converting them to polar or charged amino acid residues via site-directed mutagenesis, and the role of the proposed conformational change can be tested by locking the protein in the closed conformation via a disulfide bond; these studies are in progress.

Evidence for the conformational flexibility has been provided by the observation that small changes in temperature (10–15 deg above room temperature) lead to large changes in the CD spectrum (N. MacKenzie, personal communication). While these thermal changes may not be relevant to the structural changes attendant to binding to the lipid surface, they do show that apoLp-III has considerable secondary structural flexibility, most likely at the hinge regions.

As previously noted, the amino acid sequence of apoLp-III has many regions with a high potential to form amphipathic helices, a property which it shares with several of the water-

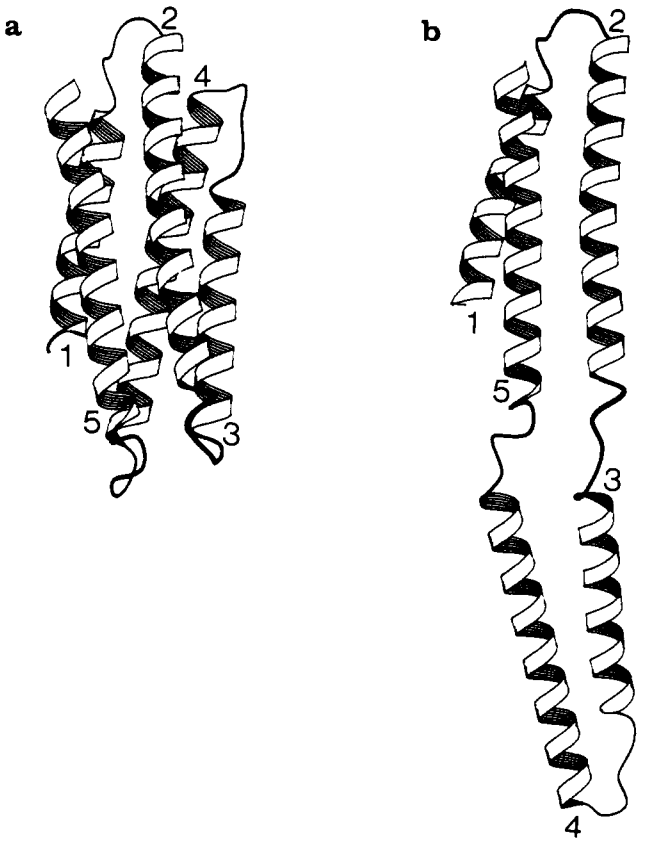

FIGURE 5: Ribbon drawings of the apoLp-III structure in folded and unfolded form. (a) A ribbon drawing representing the apoLp-III structure as seen in the crystalline state is shown. Each helix is labeled by number according to the nomenclature described in the text. (b) A ribbon drawing of the putative unfolded form of the apoLp-III structure as it binds to the lipophorin particle is shown. Again, each helix is labeled as described.

soluble mammalian apolipoproteins (Cole et al., 1987; Kanost et al., 1988). In addition, the insect and mammalian proteins all have CD spectra which are consistent with a high content of α-helix (Boguski et al., 1986). If these mammalian proteins have tertiary structures similar to that of apoLp-III, i.e., with the hydrophobic residues sequestered in the interior of helical bundles, then the model proposed here for the binding of the insect protein to lipid surfaces may well apply to the mammalian proteins. One difference between the insect and mammalian apolipoproteins, however, is the presence of proline repeats every 22 amino acids in many of the mammalian molecules. It may mean that either the lengths of the helical regions are significantly shorter in the mammalian proteins or rather may simply reflect an insertion of a proline residue in an otherwise helical segment as seen in helix 4 of the locust apoLp-III. Regardless of the positions of the prolines in the mammalian proteins, the general principle of a water-soluble apolipoprotein unfolding on the lipid surface to expose its hydrophobic interior is still applicable.

ACKNOWLEDGMENTS

We thank Drs. W. W. Cleland, David Eisenberg, Bill Montfort, and Jere Segrest for helpful discussions, Dr. Gerry Wyatt for samples of locust hemolymph, and Dr. Robert Sweet for assistance at the National Synchrotron Light Source, Beam Line 13C, Brookhaven National Laboratory.

REFERENCES

Abad-Zapatero, C., Griffith, J. P., Sussman, J. L., & Rossmann, M. G. (1987) *J. Mol. Biol. 198*, 445–467.

Blum, M., Metcalf, P., Harrison, S. C., & Wiley, D. C. (1987) *J. Appl. Crystallogr. 20*, 235–242.

Boguski, M. S., Freeman, M., Elshourbagy, N. A., Taylor, J. M., & Gordon, J. I. (1986) *J. Lipid Res. 27*, 1011–1034.

Chino, H., & Yazawa, M. (1986) *J. Lipid Res. 27*, 377–385.

Chino, H., Downer, R. G. H., Wyatt, G. R., & Gilbert, L. I. (1981) *Insect Biochem. 11*, 491.

Cole, K. D., Fernando-Warnakulasuriya, G. J. P., Boguski, M. S., Freeman, M., Gordon, J. I., Clark, W. A., Law, J. H., & Wells, M. A. (1987) *J. Biol. Chem. 262*, 11794–11800.

Eisenberg, D., Wesson, M., & Wilcox, W. (1989) *Prediction of Protein Structure and the Principles of Protein Conformation*, pp 635–646, Plenum Publishing Corp., New York.

Hendrickson, W. A., & Ward, K. B. (1977) *J. Biol. Chem. 252*, 3012–3018.

Holden, H. M., Kanost, M. R., Law, J. H., Wells, M. A., & Rayment, I. (1988) *J. Biol. Chem. 263*, 3960–3962.

Jones, T. A. (1985) *Methods Enzymol. 115*, 157–171.

Kanost, M. R., McDonald, H. L., Bradfield, J. Y., Locke, J., & Wyatt, G. R. (1987) in *Molecular Entomology* (Law, J., Ed.) pp 275–283, Alan R. Liss, Inc., New York.

Kanost, M. R., Boguski, M. S., Freeman, M., Gordon, J. I., Wyatt, G. R., & Wells, M. A. (1988) *J. Biol. Chem. 263*, 10568–10573.

Kanost, M. R., Kawooya, J. K., Law, J. H., Ryan, R. O., Van Heusden, M. C., & Ziegler, R. (1990) *Adv. Insect Physiol. 22*, 298–396.

Kawooya, J. K., Keim, P. S., Ryan, R. O., Shapiro, J. P., Samaraweera, P., & Law, J. H. (1984) *J. Biol. Chem. 259*, 10733–10737.

Kawooya, J. K., Meredith, S. C., Wells, M. A., Kezdy, F. J., & Law, J. H. (1986) *J. Biol. Chem. 261*, 13588–13591.

Mathews, F. S., Levine, M., & Argos, P. (1972) *J. Mol. Biol. 64*, 449–464.

Richardson, J. (1981) *Adv. Protein Chem. 34*, 167–339.

Rossmann, M. G. (1960) *Acta Crystallogr. 13*, 221–226.

Rossmann, M. G. (1979) *J. Appl. Crystallogr. 12*, 225–238.

Schmid, M. F., Weaver, L. H., Holmes, M. A., Grutter, M. G., Ohlendorf, D. H., Reynolds, R. A., Remington, S. J., & Matthews, B. W. (1981) *Acta Crystallogr. A37*, 701–710.

Segrest, J. P., Jackson, R. L., Morrisett, J. D., & Gotto, A. M., Jr. (1974) *FEBS Lett. 38*, 247–253.

Shapiro, J. P., Keim, P. S., & Law, J. H. (1984) *J. Biol. Chem. 259*, 3680–3685.

Shapiro, J. P., Law, J. H., & Wells, M. A. (1988) *Annu. Rev. Entomol. 33*, 297–318.

Terwilliger, T. C., & Eisenberg, D. (1983) *Acta Crytallogr. A39*, 813–817.

Tronrud, D. E., Ten Eyck, L. F., & Matthews, B. W. (1987) *Acta Crystallogr. A43*, 489–501.

Van der Horst, D. J., Van Doorn, J. M., & Beenakkers, A. M. T. (1984) *Insect Biochem. 14*, 495–504.

Weber, P. C., Bartsch, R. G., Cusanovich, M. A., Hamlin, R. C., Howard, A., Jordon, S. R., Kamen, M. D., Meyer, T. E., Weatherford, D. W., Xuong, N. H., & Salemme, F. R. (1980) *Nature (London) 286*, 302–304.

Wells, M. A., Ryan, R. O., Kawooya, J. K., & Law, J. H. (1987) *J. Biol. Chem. 262*, 4172–4176.